Cold Regions Science and Technology 111 (2015) 39–48

Contents lists available at ScienceDirect

Cold Regions Science and Technology

journal homepage: www.elsevier.com/locate/coldregions

Imaged brine inclusions in young sea ice—Shape, distribution and formation timing

R.J. Galley [a,*], B.G.T. Else [e], N.-X. Geilfus [c], A.A. Hare [a], D. Isleifson [a,d], D.G. Barber [a], S. Rysgaard [a,b,c]

[a] Centre for Earth Observation Science, University of Manitoba, 125 Dysart Road, Winnipeg, Manitoba, Canada, R3T 2N2
[b] Greenland Climate Research Center, Greenland Institute of Natural Resources, Kivioq 2, P.O. Box 570, 3900 Nuuk, Greenland
[c] Department of Bioscience, Arctic Research Centre, Aarhus University, 8000 Aarhus C, Aarhus, Denmark
[d] Department of Electrical Engineering and Computer Engineering, University of Manitoba, 75 Chancellor's Circle, Winnipeg, Manitoba, Canada, R3T 2N2
[e] Department of Geography, University of Calgary, 2500 University Dr. NW, Calgary, Alberta, Canada, T2N 1N4

ARTICLE INFO

Article history:
Received 5 August 2014
Received in revised form 19 November 2014
Accepted 20 December 2014
Available online 24 December 2014

Keywords:
Arctic
Sea ice
Brine channels
Magnetic resonance imaging
Brine volume

ABSTRACT

Liquid inclusions in sea ice are variable and dependent on the myriad of physical conditions of the atmosphere–sea ice environment in which the sea ice was grown, and whether or not melting processes affected the sea ice. In that light, there exist relatively few observations and resultant quantification of the morphology and vertical distribution of brine inclusions in sea ice. Using a magnetic (3.0 T) resonance (MR) imager using constructive interference steady state gradient echo sequence, we show that it is possible to image brine channels and pockets in an 18.5 cm young sea ice core in three-dimensions in only four and a half minutes following core storage at −20 °C. We present a three-dimensional image of a brine drainage channel feature in a young sea ice core, give the physical context for its formation by presenting the physical conditions of the atmosphere and water/sea ice prior to sea ice growth through the sampling date, and observe its physical characteristics. We illustrate that brine drainage channels may be established concurrently with ice growth, and indicate the amount and location of vertical and horizontal fluid connectivity in the young sea ice sample in the context of the environment in which it grew. Finally, we show that a vertical brine volume distribution profile can be calculated using MR image data, extending the (non-imaging) nuclear magnetic resonance work of others in this vein.

1. Introduction

The crystal structure of sea ice and its inclusions control its mechanical strength (Assur, 1960), and its ability to exchange heat, salt and radiation (Light et al., 2003), which in turn affect the atmosphere above and the ocean below, physically, chemically (Vancoppenolle et al., 2013) and biologically (Fritsen et al., 1994; Krembs et al., 2000). The apparent optical properties of sea ice are contingent on the distribution of gas and liquid inclusions and the electromagnetic properties of sea ice are governed by the size, shape, and orientation of these inclusions. Therefore, improved knowledge of these properties is required for interpreting sea ice scattering signatures obtained using remote sensing techniques (Tucker et al., 1992). Liquid inclusions in sea ice largely determine the volumes' heat capacity and permeability (e.g. Golden et al., 1998, 2007; Weeks and Ackley, 1982), which controls bulk flow in the volume and may act to flood the sea ice surface from below, or drain the sea ice volume to the ocean (e.g. Vancoppenolle et al., 2007). Brine drainage channels are very important, as they are likely the sites of the bulk of the liquid convection (i.e. gravity drainage) to the sea ice-seawater interface (Eide and Martin, 1975; Lake and Lewis, 1970; Niedrauer and Martin, 1979; Notz and Worster, 2008; Oertling and Watts, 2004; Untersteiner, 1968; Weeks and Ackley, 1986). Notz and Worster (2009) conclude that brine drainage is governed by the sea ice thickness, permeability, and the established brine density gradient.

Observations by Bennington (1967) using ice samples 50 cm (December), 120 cm (January) and 160 cm (February) thick over the winter of 1964/1965 indicate that brine drainage channels formed during ice growth (termed first-generation drainage channels) are conically shaped, interconnected networks of brine pockets between platelets; a second type of channel with similar morphology is characteristic of melting sea ice (termed second-generation brine drainage channels). Lake and Lewis (1970) showed that sea ice near the seawater interface was partly composed of vertical tubular structures attended at angles of 40°–54° by smaller tributary channels which often followed crystal boundaries (sample thickness = 155 cm). That range of angles was later expanded to 30°–60° by Niedrauer and Martin (1979) in microcosm experiments with NaCl ice, and corroborated by Kovacs (1996) and Cole and Shapiro (1998) in medium and thick first year ice. These 'starburst patterns' when looked on from above, had a mean diameter of 4 cm and the individual feeder channels were 2–3 cm long and 2–8 mm in diameter (Lake and Lewis, 1970), indicating the potential for horizontal brine movement within sea ice toward preferred vertical drainage areas, though no mention was made of when or how fast

* Corresponding author.
E-mail address: ryan.galley@ad.umanitoba.ca (R.J. Galley).

http://dx.doi.org/10.1016/j.coldregions.2014.12.011
0165-232X/

they formed. Lake and Lewis (1970) also found the largest, most well developed inclusions in the bottom 20 cm of their ice samples (13 % of a 1.55 m sample thickness), noting that higher, diffuse structures were most likely remnants left by past ice growth.

More recently, the model of Wells et al. (2011) tested against the experimental results of Wettlaufer et al. (1997) predicts regions of low solid fraction close to brine channel walls where feeder channels were observed by Lake and Lewis (1970). This suggests that the exchange of liquid between ocean and sea ice occurs by convective brine drainage, which was also observed in freezing sucrose solutions by Aussilous et al. (2006) and by Notz and Worster (2009) using bulk sea ice electrical impedance measurements.

Eicken et al. (2000) used MR imaging as a method for the characterization of the microstructural evolution of sea ice inclusions. The authors presented sequential images of horizontal thin sections as they warmed, though individual samples took between four and 12 hours and required the use of temperature controlled infrastructure in the MR imager (Eicken et al., 2000). Using Nuclear Magnetic Resonance (NMR), Mercier et al. (2005) showed isotropy and anisotropy in sea ice diffusion coefficients. Callaghan et al. (1999) and Hunter et al. (2009) showed the NMR technique well-replicated calculated brine volume fractions in sections of Antarctic sea ice up to 220 cm thick and 180 cm thick respectively. However, the NMR technique is unable to determine pore sizes, shapes, or distribution within the sea ice, highlighting the need for a greater library of physical observations of liquid inclusions in sea ice under a variety of sea ice types/environments (e.g. Hunke et al., 2011).

Here we endeavour to add a three-dimensional image of a brine drainage channel feature in young sea ice (18.5 cm thick) to the literature using an imaging sequence that was performed with a standard human MR imager in as little as 4 min and 30 s. We present observations of the physical characteristics of the brine drainage channel, and discuss the atmospheric, seawater, and sea ice conditions under which it formed. Finally, we present a vertical brine volume distribution profile of our sea ice sample using MR image data to extend the (non-imaging) nuclear magnetic resonance work of others.

2. Methods

In December 2011 and January 2012, a sea ice growth experiment was conducted at the Sea-ice Environmental Research Facility (SERF) at the University of Manitoba. The SERF is an 18.2 m (length) by 9.1 m (width) by 2.75 m (depth) outdoor pool filled with artificial seawater similar in composition to natural average seawater (see Hare et al., 2013 for a chemical analysis of the seawater composition, after Millero, 2006). Impurities of course occurred in the commercial salts used to formulate the seawater, and those left undissolved could be seen suspended in the water column at the beginning of the experiment. The experiment began on 22 December 2011 by allowing the pool to cool by turning off its heating system. The sea ice in the SERF was initially allowed to form in the absence of wind forcing and snow accumulation to ensure uniform ice formation and growth over the entire pond area (~165 m^2) using the facility's retractable roof to shield the ice surface. Though the sea ice was initially grown in the absence turbulent forcing, the conditions under which it formed yielded young sea ice that was physically and chemically similar to natural Arctic sea ice (e.g. Geilfus et al., 2013b; Hare et al., 2013; Rysgaard et al., 2014).

The 2-m air temperature over the pool surface was recorded using a Vaisala HMP45C probe enclosed in a radiation shield connected to an automated station logger. Seawater and later sea ice and seawater temperatures through the depth of the pool were measured by the same automated station using type-T thermocouples (Omega Engineering, USA) placed in the pool at 5 cm intervals from 0 to 1.2 m and at 20 cm intervals from 1.2 m to 2.4 m to show general warming and cooling timing and trends in the volume (Fig. 1).

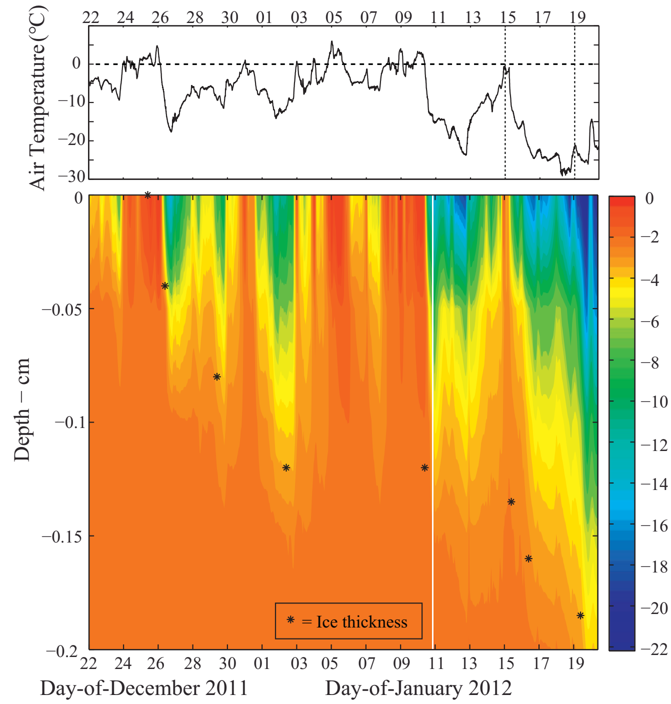

Fig. 1. (Top) 2-m air temperature and (bottom) sea ice and water temperature for the duration of the ice growth experiment overlain by ice thickness measurements. A vertical dashed line in the air temperature panel indicates two snow or blowing snow events.

No sea ice samples were taken prior to 11 January to ensure a uniform and undisturbed sea ice volume at least 10 cm thick (Fig. 2a). Sea ice samples were extracted on 11, 16 and 20 January using a Kovacs Mark II ice coring system. One core sample each day was cut into 2-cm thick sections, which were melted in sealed buckets. Bulk salinity of these sections was determined by measuring the conductivity and temperature of the melt using a Hach SensION 5 conductivity probe. These salinity data are presented with the caveat that this method may underestimate the actual bulk salinity (e.g. Notz et al. (2005)) of relatively warm young sea ice. Storage has also been shown to have an effect on sea ice bulk salinity when measured this way (e.g. Cox and Weeks, 1986) though our cores were not stored frozen and were analyzed within hours of their melting.

A second core on each date was used to determine the sea ice temperature immediately upon extraction at the mid-point of each 2 cm thickness subsample using a digital thermometer (Traceable Control Company, Model 4000, accuracy $= \pm 0.05$ °C). Pringle and Ingham (2009) propose that temperature measurements using extracted cores should be done within 5 min, noting that the accuracy of these measurements can easily be less than 0.5 °C (e.g. Eicken et al. (2004) achieved an accuracy of 0.2 °C). Using the in situ temperatures and bulk salinity data from the cores, the brine volume was calculated using the equation of Cox and Weeks (1983) assuming a density of 917 kg m^{-3} (these equations may underestimate in situ brine volume of sea ice, especially for high brine volumes and/or warm in situ sea ice temperatures due to brine loss upon core extraction). On 20 January a third core was retrieved and was immediately stored at -20 °C for MR imaging. In the absence of a method that preserves the natural temperature gradient within sea ice immediately and without change upon extraction, ex situ analysis of sea ice samples after storage at low temperatures is an established protocol. For example, Eicken et al. (2000) and Bock and Eicken (2005) based their conclusions regarding sea ice microstructural evolution with temperature under the assumption that cores stored at low (<-20 °C) temperatures then subsequently warmed as they were imaged behave similarly to sea ice in the natural system.